

## The origins of stereoselectivity in asymmetric reductions with boranes based on (+)- $\alpha$ -pinene — II. The geometries of competing transition-states and the nature of the reaction. A semiempirical study

Milorad M. Rogic,<sup>a,\*</sup> P. Veeraraghavan Ramachandran,<sup>b</sup> Herman Zinnen,<sup>c</sup> Leo D. Brown<sup>c</sup> and Manli Zheng<sup>c</sup>

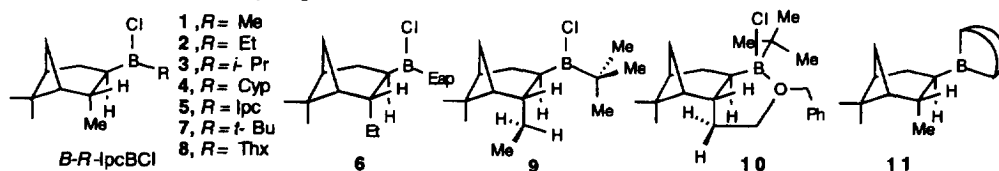
<sup>a</sup> Molecular Modeling Research Institute, St. Louis, Missouri 63131, USA

<sup>b</sup> Department of Chemistry, Purdue University, West Lafayette, Indiana 47907, USA

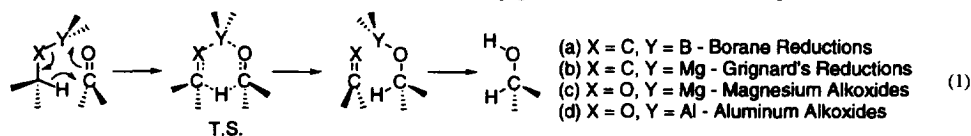
<sup>c</sup> CAChe Scientific, Beaverton, Oregon 9707, USA

**Abstract:** In the first paper from this series we pointed out that the stereoselectivity in the reduction of benzaldehyde with *B-alkyl-9*-BBN reagents greatly depends on the borane reagent conformations. The AM1 calculations show that the stereoselectivity in the reduction of acetophenone with a series of *B-lpc*-BYX reagents is also controlled by the borane conformations. It appears that this control is imposed early along the reaction coordinate, during generation of the first rather than the second of the two new transition-state's stereogenic centers, i.e. during  $B\text{-}sp^2 \rightarrow B\text{-}sp^3$ , rather than  $C\text{-}sp^2 \rightarrow C\text{-}sp^3$  process. The calculated enantiomeric excesses were generally in good agreement with the experimentally observed ones: BXY=9-BBN, (S): 99 vs. 87%; X=Cl, Y=Me, (S): 13% vs. 14.5%; Et, (S): 44% vs. 33%; *i*-Pr, (S): 84% vs. 81; Cyp, (S): 85% vs. 84%; *lpc*, (S): 99% vs. 98%; *t*-Bu, (R): 97% vs. 96%; Thx, (R): 99% vs. 83%. The reversal of absolute configuration in the reductions with *B-t*-Bu-*lpc*BCl and *B*-Thx-*lpc*BCl is a logical consequence of the reaction mechanism. Unlike in the simple nucleophilic additions to carbonyl group from the Felkin–Anh model, where the stereoselectivity is controlled by the developing steric interactions only on the single reactive prostereogenic center provided by the substrate, it appears that in the borane reductions the stereoselectivity is mainly controlled by analogous steric interactions developing on the prostereogenic boron center in the reagent. © 1997 Elsevier Science Ltd

The boranes derived from  $\alpha$ -pinene are among the most versatile reagents for the asymmetric syntheses.<sup>1</sup> The asymmetric reduction of carbonyl compounds with various reagents from this class, 1–11, have been extensively explored<sup>2–5</sup> and reviewed.<sup>1</sup>



It is believed<sup>6a</sup> that these reductions generally proceed through a cyclic, six-membered transition-state reminiscent of the Meerwein–Ponndorf–Verley processes, (MPV),<sup>6b</sup> (eq 1).



\* Corresponding author. Address for correspondence: 15 Vanessa Drive, St. Louis, MO 63131, USA; Email: MMRogic@aol.com

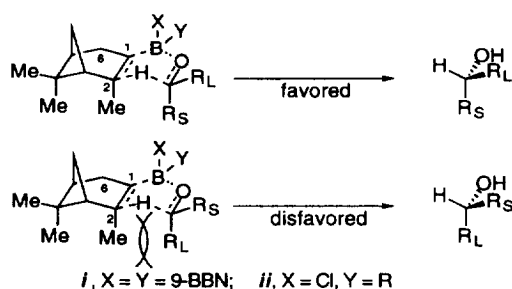


**Figure 1.** Proposed transition-state models for the reduction of aldehydes and ketones with Alpine-Borane<sup>⊕</sup> (i), and with *B*-alkyl-IpcBCl reagents (ii).

Midland introduced an analogous transition-state model, in a boat form, for the reduction of benzaldehyde with the *B*-alkyl-9-BBN reagents and invoked<sup>2b-d,3b</sup> the syn-1,3-steric interactions of the C<sub>2</sub>-Me group with the carbonyl substituents to explain the observed exclusive enantioselectivity in the reduction with the *B*-Ipc-9-BBN (Figure 1, i). A model embodying the main feature of the Midland's model, was later adopted as a tentative transition-state model for the asymmetric reductions with other borane reagents derived from  $\alpha$ -pinene<sup>3b-d,4a-f,5</sup> (Figure 1, ii).

While the model in most cases correctly predicts configuration of the predominant alcohol, there are, however, several examples where it fails.<sup>4d,5</sup>

Recently we used the AM1 Hamiltonian to reexamine the benzaldehyde reduction with Alpine-Borane<sup>⊕</sup> and other *B*-alkyl-9-BBN reagents and identified importance of the borane reagent's conformation on the stereoselectivity and overall reactivity.<sup>7</sup> Here, we report how the size of the *B*-R- group in a series of *B*-R-IpcBCl reagents (R=Me-, Et-, *i*-Pr-, Cyp-, Ipc-, *t*-Bu- and Thx-), affects the reactivity and stereoselectivity of these reagents in the reduction of acetophenone. We also explain the absolute configuration change of the alcohol in the reduction of acetophenone with the *B*-*tert*-alkyl-IpcBCl reagents,<sup>4c</sup> the Achilles' heel of the original transition-state model, and extend the Felkin-Ahn interpretation<sup>8a-d</sup> of the origin of stereoselectivity in simple nucleophilic additions to carbonyl group<sup>8e,f</sup> to this kind of reactions.

### Computational details

Semiempirical studies were carried out using AM1<sup>9</sup> method as implemented by CAChe<sup>10a</sup> release 94 of MOPAC,<sup>10b</sup> version 6, on the CAChe worksystem.<sup>10a</sup>

The required molecular geometries for chloroborane reagents and for acetophenone were generated using CAChe Molecular Editor<sup>10a</sup> and then fully optimized in MOPAC using eigenvector following.<sup>10c</sup> The two dimensional map of the rotational barriers about the B-Ipc bond was generated as before<sup>7</sup> by optimizing individual geometries resulting from the two degree torsional angle changes. Thermodynamic quantities were obtained from the calculated heats of formation of the corresponding reactants and products.

Transition-states geometries and the energies of activation were obtained using SADDLE calculation.<sup>11a</sup> The reactants and products geometries, which are on the opposite sides of the transition-states along the reaction coordinate, were first optimized. Initial transition-state geometry candidates were then generated by manually 'docking' the reducing agent and acetophenone molecules in CAChe Visualizer until their frontier orbitals just begin to overlap without steric interactions. After visual inspection of the calculated transition-state geometry, the structure was further refined by minimizing gradient using eigenvector following. For each transition-state, a vibrational spectrum calculation was carried out to verify that it had only one large negative frequency level and that this frequency was associated with the expected reaction coordinate.<sup>11c</sup> Subsequent MOPAC Intrinsic Reaction Coordinate calculations<sup>11b</sup> provided reaction coordinate maps connecting transition-state with the precursor structures (reaction intermediates), as well as with the reaction products. Individual structures

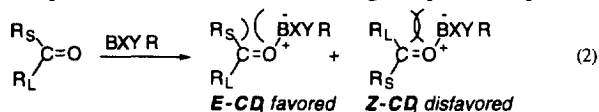
along the reaction coordinates and the corresponding potential energies were visualized and inspected using CAChe Visualizer module.

## Results and discussion

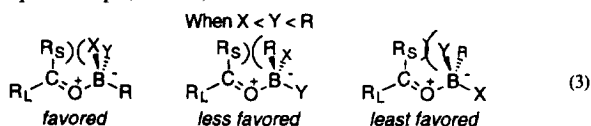
The tacit assumptions of the transition-state model in Figure 1 are (a), that all borane reagents react exclusively in a single conformation, (b), that the observed stereoselectivity for each reagent is determined by the difference in activation energies of the two diastereomeric transition-states resulting from the same conformation of the reagent, (c), that the size of the *B*-R group has no role in determining which particular conformation of the reagent will participate in the reaction, and (d), that the size of the *B*-R group has no effect on the timing of the generation of the new stereogenic centers on the original carbonyl carbon in the diastereomeric transition-state pair. In other words, according to the above transition-state model, the *B*-Ipc-9-BBN and *B*-R-IpcBCl reagents (R=*primary*, *secondary* or *tertiary* alkyl group), all should reduce acetophenone to the (*S*)-1-phenylethanol. Experimentally, however, the *B*-*tert*-alkyl-IpcBCl reagents gave the (*R*)-alcohol.<sup>4c</sup> Furthermore, in spite of the fact that according to the model the controlling syn-1,3-interactions in the transition-states for the reduction of acetophenone with the various *B*-R-IpcBCl reagents should have been essentially the same, the experimentally determined stereoselectivities were quite different.<sup>4c</sup> These and other observations<sup>5b</sup> imply that some other factors, not included in the original model, contribute to the enantioselectivity control.

### General stereochemical and mechanistic considerations

To a prochiral ketone  $R_S COR_L$ , a general boron reactant  $BRXY$  derived from  $\alpha$ -pinene (R=Ipc, XY=9-BBN, or X=Cl, Y=alkyl), appears as a Lewis acid and the initial interactions therefore should lead to a mixture of the respective *E*-CD and *Z*-CD charge-dipole complexes<sup>2a-c,4a,6a</sup> (eq 2).



Presumably, *E*-CD/*Z*-CD ratio should reflect the syn-1,2-steric interactions of the O-B bond with the C-R<sub>S</sub> and C-R<sub>L</sub> bonds<sup>9f</sup> resulting from the two alternate approaches of the ketone. In the simplest case, the ketone would encounter weakest resistance when the approach trajectory would lead to the formation of the new B-O bond where the smaller carbonyl R<sub>S</sub> substituent would be gauche to the B-X and B-Y bonds (eq 3, R=Ipc, X≤Y).

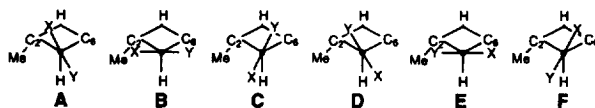


But since the opposing interactions, even in this simple case, would also include intramolecular interactions developing among the atoms of the reactants while their prostereogenic B-sp<sup>2</sup> and C-sp<sup>2</sup> centers are undergoing coordination expansion to B-sp<sup>3</sup> and C-sp<sup>3</sup> (e.g. between atoms of the Ipc ring and the X and Y groups on the one hand, and the atoms of the R<sub>S</sub> and R<sub>L</sub> substituents on the other), the *actual most preferred orientation* of the reactants will be determined by *all intermolecular as well as intramolecular interactions that would affect formation of the first new bond*. Furthermore, since only those approach trajectories where the C<sub>2</sub>-H of the Ipc group could appear either above or below the R<sub>S</sub>-C-O-B plane can lead to the product, the most favored approach trajectory in eq 3 will be a nonproductive one.

### The approach trajectories and calculated geometries of the reacting species

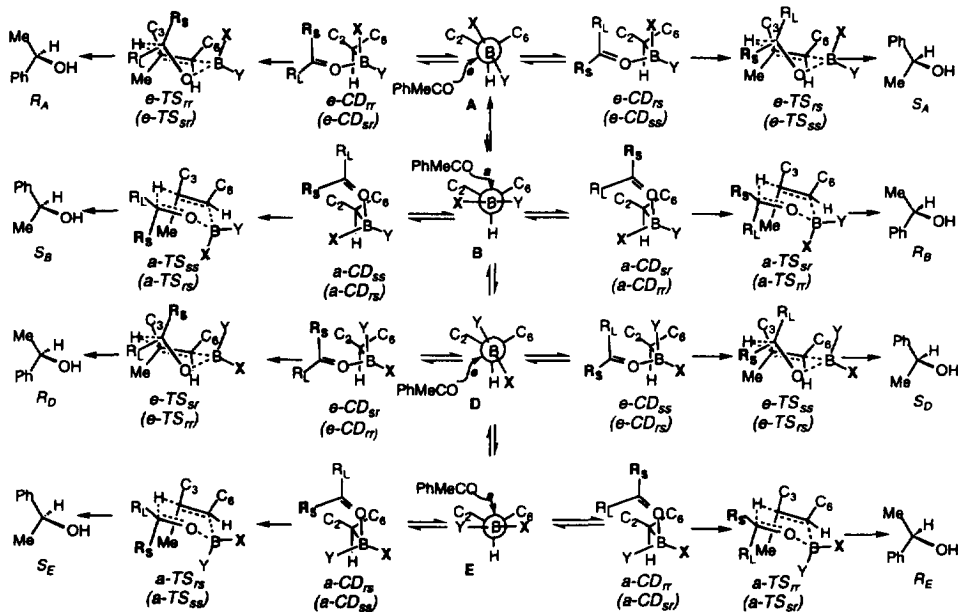
Since the carbonyl compound must approach the boron center of the *B*-Ipc-borane reagent from the same side of the B-sp<sup>2</sup> plane occupied by the C<sub>2</sub>-H hydrogen source of the Ipc ring,<sup>12a</sup> the most effective approach should take place from the directions opposite either to the C<sub>1</sub>-C<sub>6</sub> or to the C<sub>1</sub>-H

bond of the Ipc ring, but not from the direction opposite to the C<sub>1</sub>–C<sub>2</sub> bond.<sup>12b</sup> Presumably, the final geometries of these reacting conformations will be derived from the **A** and **B** of the six unique conformations<sup>13a</sup> shown in Scheme 1. It should also be remembered that unlike simple nucleophiles without a reactive prostereogenic center, which in a reaction with prostereogenic carbonyl substrate can provide only a pair of diastereomeric reaction pathways, the borane reagents can provide with the same substrate, depending on whether the boron center is prostereogenic or prochiral, either four or eight possible reaction pathways leading to four or eight diastereomeric transition-states (*vide infra*).



Scheme 1.

With this in mind, the above two principal approach trajectories of a general carbonyl substrate R<sub>S</sub>COR<sub>L</sub> to the B-sp<sup>2</sup> center of a general BIPCXY reagent could provide eight diastereomeric pathways summarized in Scheme 2. Since the semiempirical AM1 Hamiltonian<sup>9</sup> reproduces the X-ray crystal structure of the Ipc<sub>2</sub>BCl<sup>4c</sup> reasonably well, we used the AM1 first, to evaluate relative conformational stabilities in a series of the *B*-Ipc-BYX reagents, second, to calculate geometries<sup>11a-c</sup> of the diastereomeric charge–dipole complex/transition-state pairs in the reaction with acetophenone (CD/TS pairs), and finally, we used this information to determine the overall most preferred reaction pathway for each reagent.



**Scheme 2.** The subscripts describe the configurations of the original prostereogenic boron and carbonyl carbon centers, respectively. When X=Y, the **D** and **E** are degenerate and in those cases the subscripts describing the boron's configuration are meaningless, e.g. e-TS<sub>ss</sub> and e-TS<sub>ss</sub> are the same as e-TS<sub>s</sub>. However, when X≠Y, the boron's subscripts in the configuration labels depend on the nature of the Y substituent; the labels in parentheses refer to *tert*-R.

#### *The most stable and the reacting conformations of the borane reagents*

The geometries of the calculated most stable conformations of the *B*-Ipc-9-BBN and all *B*-R-IpcBCl reagents, together with their calculated heats of formation, H<sub>f</sub>, are shown in Figure 2.<sup>14a</sup> The structure

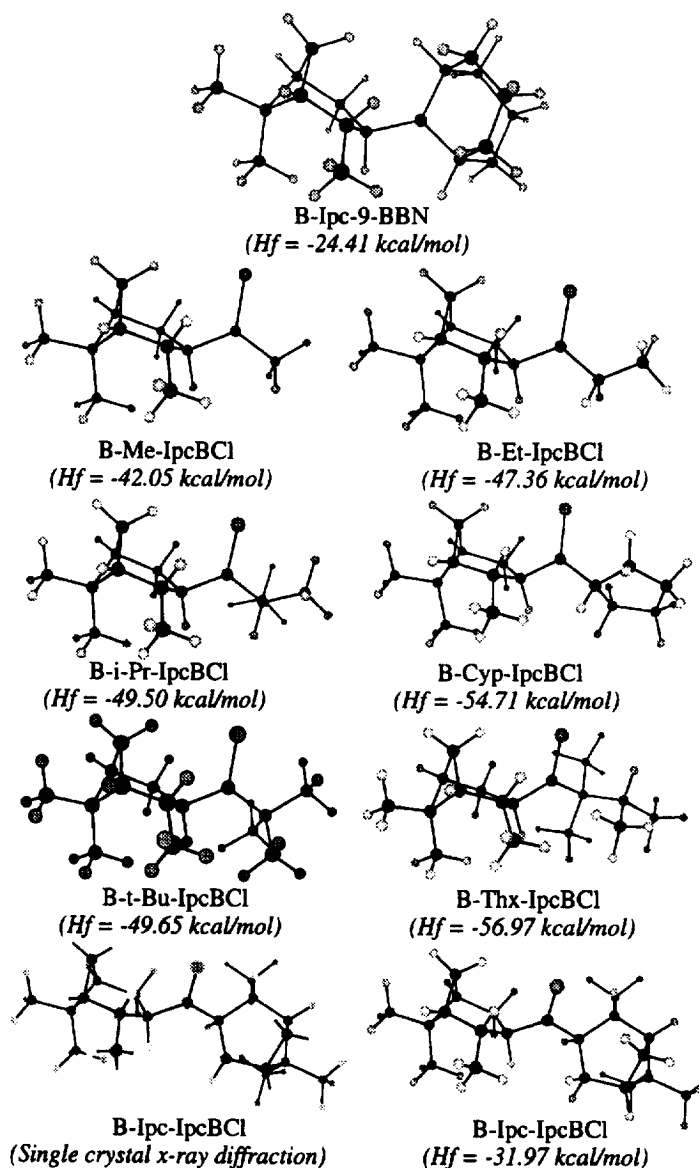


**Figure 2.** Calculated geometries and heats of formation of the most stable conformations of the *B*-Ipc-9-BBN and *B*-R-IpcBCl reagents, and the structure of Ipc<sub>2</sub>BCl from the single crystal X-ray analysis.

of the Ipc<sub>2</sub>BCl from the single crystal X-ray analysis<sup>4c</sup> is also included. Figure 3 shows the changes in the calculated heats of formation of all *B*-IpcBXY agents as a function of the Y–B–C<sub>1</sub>–H torsional angle during rotation of the X–B–Y group about the B–Ipc bond.

According to Figure 3, during the A to B rotations of the *B*-alkyl-IpcBCl reagents, with the exception of the *B*-Me-IpcBCl, the B conformations and most of the A ones appear to be ‘local’ rather than ‘global’ energy minima.<sup>13</sup> Moreover, the intermediate conformations on the potential energy curves resulting from the B–Cl and C<sub>1</sub>–C<sub>2</sub> bonds eclipsing, do not appear as the energy maxima. The *B*-*t*-Bu-IpcBCl case illustrates the point (see Figure 3). During rotation from A to B, as the B–Cl bond moves to eclipse the C<sub>1</sub>–C<sub>2</sub> bond, the much larger *t*-Bu group begins to move toward the C<sub>1</sub>–C<sub>6</sub>

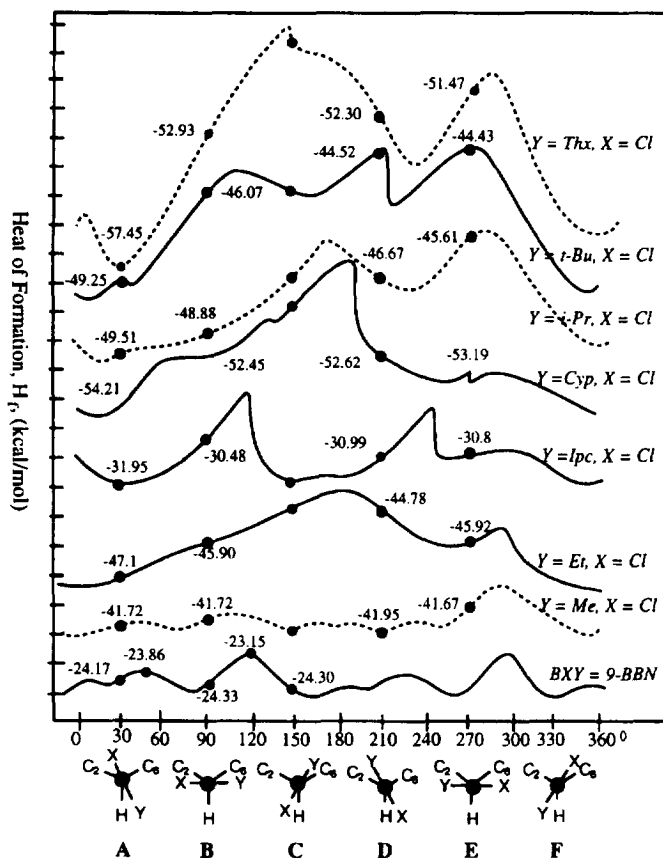


**Figure 3.** Calculated barriers for rotation of the X–B–Y group about the Ipc–B bonds in *B*-Ipc-9-BBN and *B*-R-IpcBCl reagents (as heats of formation in kcal/mol). The H<sub>1</sub> are offset from each other as indicated at the origin of the curves. Individual points on each curve correspond to the A, B, C, and D, E, F conformations. The HE<sub>1</sub> and HE<sub>2</sub> points on the *B*-Ipc-9-BBN curve identify the barriers for the rotation between A and B and B and C conformations.

bond. Even after the B–Cl bond had eclipsed the C<sub>1</sub>–C<sub>2</sub> bond and when it begins to move away from the C<sub>1</sub>–C<sub>2</sub> bond, the *B*-*t*-Bu bond will continue to move toward the C<sub>1</sub>–C<sub>6</sub> bond. As a consequence, the steric interactions between the *B*-*t*-Bu group and the C<sub>1</sub>–C<sub>6</sub> bond opposing the rotation — and thus the torsional energy required to overcome this resistance — will continue to increase. Evidently, contribution of the B–Cl/C<sub>1</sub>–C<sub>2</sub> bond eclipsing to the torsional energy is masked by the increase in steric energy<sup>14b</sup> apparently arising from the stronger interactions between the C<sub>1</sub>–C<sub>6</sub> and the B–R bonds as well as from the other interactions among atoms distant in sequence but close in space, not conveniently depicted in the schematic representations such as Scheme 1. It appears that the calculated energies for forcing *B*-R-IpcBCl molecules from the conformation A into conformation B increase in order Me < *i*-Pr < Et < Ipc < Cyp < *t*-Bu < Thx.

The above results suggest that during the reaction the geometries of the reactant's starting conformations in the first diastereomeric bimolecular reaction intermediates, i.e. the geometries of the reagent's and substrate's components in the resulting CD complexes, will be already different than their starting geometries. Nevertheless, as long as the relative energies of the starting A and B conformations of the *B*-IpcBXY are known, their contributions to the competing reaction pathways can be evaluated.<sup>13c</sup>

### Calculated geometries of the CD complexes and transition-states

Using the *B-t-Bu-IpcBCl*/acetophenone reaction as an example, Figure 4 illustrates the calculated geometries of the CD/TS pairs resulting from the two principal approaches mentioned above. The approach from the direction opposite to the C<sub>1</sub>–C<sub>6</sub> bond of the Ipc ring in the conformation **A**, i.e. from a general equatorial side of the Ipc ring, would provide the e-CD complexes and e-TS transition-states. The approach from the direction opposite to the C<sub>1</sub>–H bond of the Ipc ring in the **B** conformation, i.e. from a general axial side of the Ipc ring, provides the a-CD/a-TS pair. (See footnote g in Table 2 and note the other possible arrangements of the boron's and carbonyl carbon's *Re* and *Si* faces corresponding to reaction with **D** and **E** conformations from Scheme 2. In the case of the *B-t-Bu-IpcBCl* reagent, the four pathways from **D** and **E** are substantially higher in energy due to the unfavorable syn-1,3-interactions among the R<sub>L</sub> (=phenyl), R<sub>S</sub> (=Me) and Y (=t-Bu) groups, and are ignored. However, in other cases where Y (=primary alkyls) is comparable in size to X, their contribution should not be ignored.) The calculated geometries and the energies are shown (together with calculated structures from the Ipc<sub>2</sub>BCl/acetophenone reaction) in Figure 5.

#### (a) CD Complexes

Calculated geometries of the CD complexes (Figs 4 and 5) clearly show (a), that the formation of the new O–B bond between the reactants is accompanied by appropriate pyramidalization at the boron center in the reagent component of the system (and other geometrical changes, e.g. note the ω<sub>R</sub> in the starting **A** and **B** conformations and in the resulting CD/TS pairs), and (b), that at this stage of reaction, *with the exception of the phenyl ring's conformation relative to the carbonyl C-sp<sup>2</sup> plane*, the carbonyl carbon pyramidalization in the carbonyl component of the system still did not start to take place<sup>15</sup> (i.e. in all CD complexes the Θ<sub>CO</sub> was essentially 0°, but in order to avoid severe steric interactions of one of the *ortho*-hydrogens with the B–X bond, the phenyl ring had to rotate out of the plane with the carbonyl group. In general, it is the interaction of the B–X and B–C<sub>1</sub> bonds in the reagent with the R<sub>L</sub> group of the incoming ketone that determines which of the alternate B-sp<sup>2</sup> to B-sp<sup>3</sup> coordination expansion processes will take place). Additionally, the geometries of the O–B–C<sub>1</sub>–C<sub>6</sub> bonds in the e-CD complexes and of the O–B–C<sub>1</sub>–H bonds in the a-CD complexes corroborate that these complexes indeed originated from the reagent's **A** and **B** conformations as indicated in Figure 4.

#### (b) Transition-states

According to the calculated geometries of the e-TS and a-TS transition-states from Figs 4 and 5, the e-TS structures resemble a half-chair,<sup>13b</sup> where the oxygen in the C–O–(B)–C<sub>1</sub>–C<sub>2</sub> sequence and the hydrogen at the C<sub>2</sub> appear below and above the plane occupied by the C<sub>2</sub>–C<sub>1</sub>–B atoms. Here, the pseudoaxial B–X bond appears *trans* to the C<sub>1</sub>–H bond while the B–O bond is *trans* to the C<sub>1</sub>–C<sub>6</sub> bond of the Ipc ring (see e-TS in Figure 4). On the other hand, the a-TS structures are apparently flattened chairs where the C–O and C<sub>1</sub>–C<sub>2</sub> bonds are almost in the same plane; here, the axial B–X bond is *cis* to the C<sub>1</sub>–H and the O–B bond is *trans* to the C<sub>1</sub>–H.

The principal feature of the all CD/TS pairs is that the B–O bond is formed by the coordination of the oxygen's in-plane n electron pair to the boron center,<sup>15,16</sup> rather than the π-electrons as implied by the boat transition-states in Figure 1. Note the relative changes in the ω<sub>R</sub>, ω<sub>1</sub> and ω<sub>2</sub> torsional angles in all reaction pathways.

#### Preferred diastereomeric reaction pathways

As mentioned in the Introduction, the original interpretation of the acetophenone reduction with the borane reagents **1–11** predicts the reaction pathway leading to the (*S*)-alcohol *via* a boat-like, six-membered transition-state, to be the predominating one (see Figure 1).

Tables 1 and 2 show the calculated and observed enantioselectivities and other relevant information for all the reactions, but we will discuss in some detail only the reductions with the *B-Ipc-9-BBN*, *B-Ipc-IpcBCl*, and with *B-t-Bu-IpcBCl* reagents. The appropriate energy changes for these three

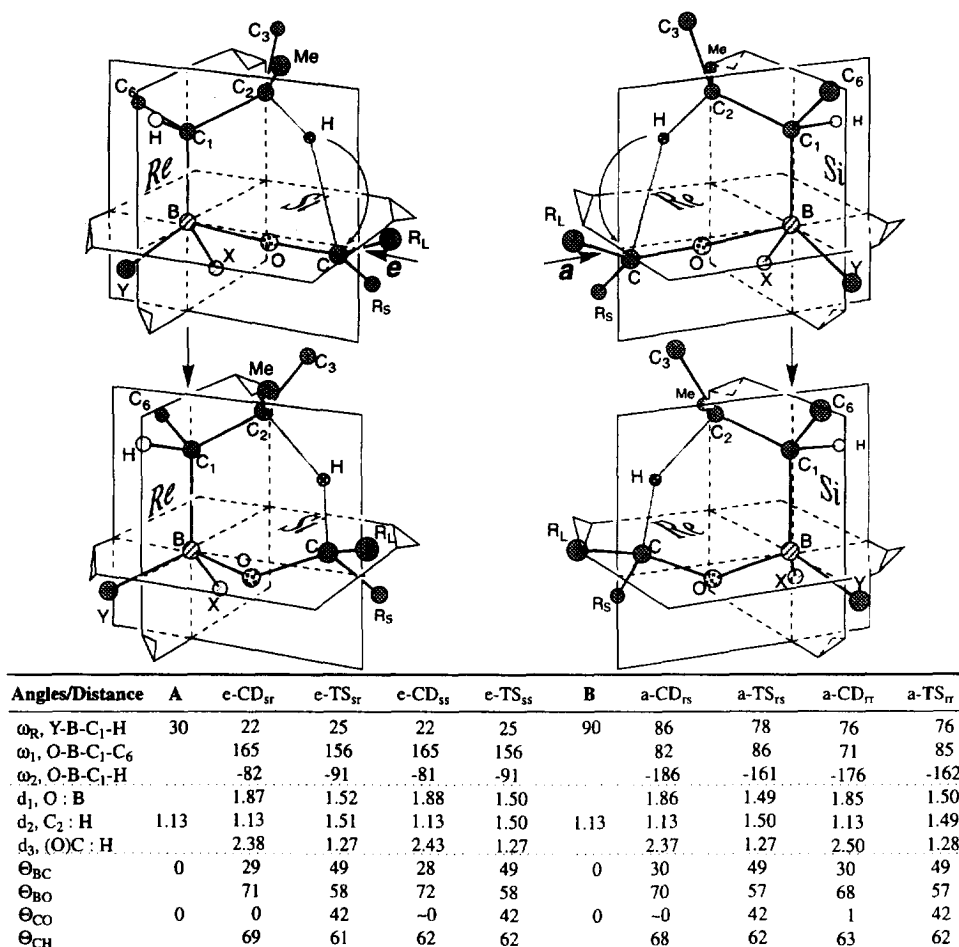


**Figure 4.** The geometries of the two principal trajectories for a prochiral carbonyl compounds approach to the B- $sp^2$  center of a B-IpcBXY reagent leading to the pair of diastereomeric complexes and transition-states. The approach from the direction opposite to the C<sub>1</sub>-C<sub>6</sub> bond, the *e-approach*, provides the e-CD and e-TS (on the left), and the approach from the direction opposite to the C<sub>1</sub>-H bond, the *a-approach*, provides the a-CD and a-TS (on the right). The curved arrows indicate the rotations about the B-C bond required to bring the C<sub>2</sub>-H close to the carbonyl carbon and to push the CD complex to the corresponding transition-state. Only the C<sub>1</sub>, C<sub>2</sub>, C<sub>3</sub>, and C<sub>6</sub> carbons of the Ipc ring are shown. Note the other possible arrangements of the boron's and carbonyl carbon's *Re* and *Si* faces. The calculated geometrical parameters (torsional angles,  $\omega$ , pyramidalization,  $\Theta$ , and atom distances,  $d$ , in degrees and Ångstroms) are for the reaction of the *B-t-Bu-IpcB*Cl with acetophenone (i.e. Y=*t*-Bu, X=Cl). The pyramidalization at the boron center is defined as the angles of the B-C<sub>1</sub> and B-O bonds relative to the original B- $sp^2$  plane; similarly, pyramidalization at the carbonyl carbon is defined as the angles of the O-C and C-H bonds relative to the original plane of the carbonyl group.

reactions are summarized in Figure 6. The equilibrating constants,  $K_{ab}$ , between the two reacting conformations A and B in Table 2 are calculated as mentioned above, and the heat of formation values for the reactants are sums of the heats of formation of acetophenone and the starting conformation. The heats of formation of the respective CD/TS pairs — calculated as before — are followed by the corresponding calculated enthalpy changes and the rate-constant equivalents of the activation energies.

Reaction Scheme 3 is a simplified kinetic variant<sup>17</sup> of the general reaction Scheme 2. According to the Curtin-Hammett principle<sup>18a,b</sup> and to kinetic analyses due to Winstein-Holmes<sup>18c</sup> and Elel and Ro,<sup>18d</sup> as long as the rates of the equilibration,  $k_{ab}$  and  $k_{ba}$ , between the reacting conformations A and B are much faster than the specific rates  $e-k_{rr}$ ,  $e-k_{rs}$ ,  $a-k_{sr}$ , and  $a-k_{ss}$ , leading to the



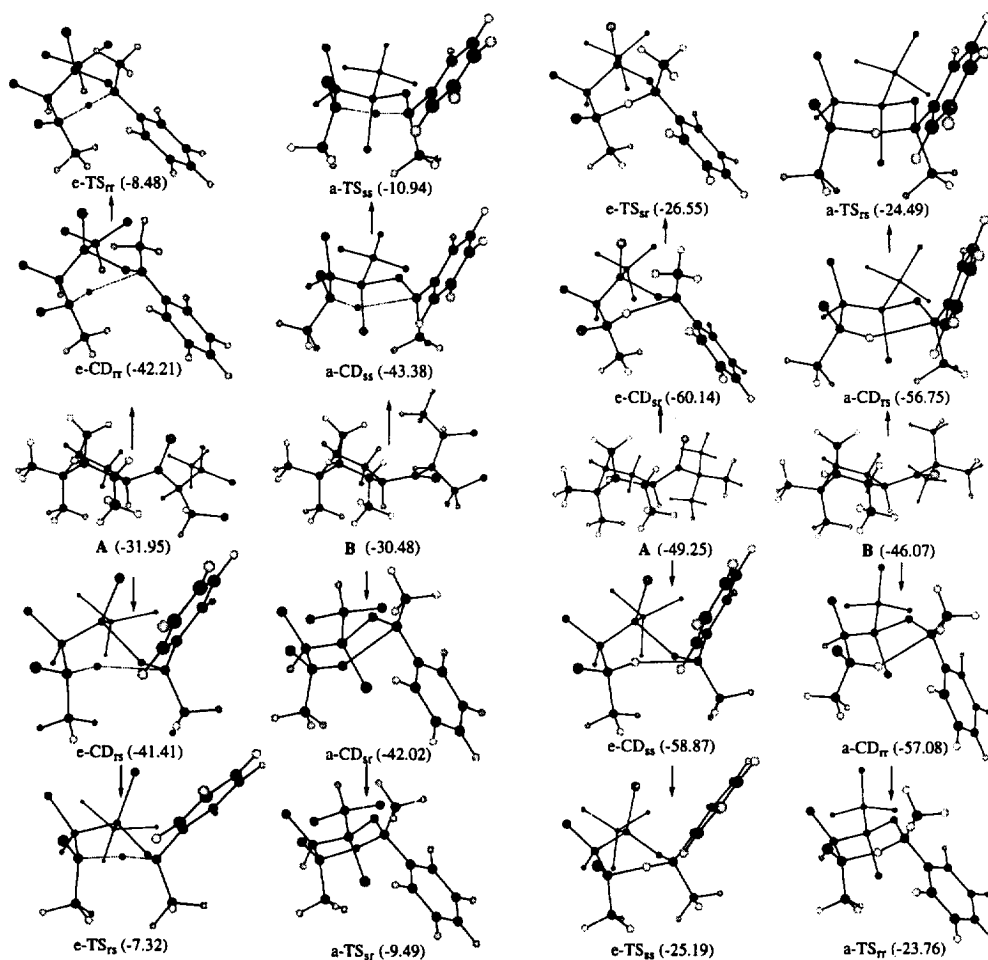


**Figure 5.** Calculated geometries of the charge-dipole complexes (CD), and the transition-states (TS), for the reduction of acetophenone with the *B-Ipc-IpcBCl* (on the left), and *B-t-Bu-IpcBCl* (on the right). Only C<sub>1</sub>, C<sub>2</sub>, C<sub>3</sub>, and C<sub>6</sub> carbons of the reacting Ipc group and the C<sub>1</sub>, C<sub>2</sub> and C<sub>6</sub> carbons of the second Ipc group, or C-Me groups of the *t*-Bu group are shown. Values in parentheses are the corresponding heats of formation (in kcal/mol). Note the syn-1,3-relationship between the B-Cl and C-Me or C-Ph bonds and the difference in orientation of the phenyl ring relative to the sp<sup>2</sup>-plane of the original carbonyl group in the more stable and less stable CD and TS pairs. Transition-states resulting from the A conformations are in a half-chair form, those resulting from the B conformations are in a flattened-chair form. The analogous geometries for the reductions with the other reagents are similar.

diastereomeric transition-states and reaction products S and R, the product ratio  $[S]_{\infty}/[R]_{\infty}$  at the end of the reaction (where  $[S]_{\infty} = ([S_A] + [S_B])_{\infty}$  and  $[R]_{\infty} = ([R_A] + [R_B])_{\infty}$ ), can be determined from the familiar expressions  $[S]_{\infty}/[R]_{\infty} = k_{SS}K/k_{rr}$ , (eq 4), or in terms of the activation energies,  $[S]_{\infty}/[R]_{\infty} = e^{-\Delta G_{TS}^{\ddagger}/RT}$ , (eq 4a), where the  $\Delta G_{TS}^{\ddagger}$  is the difference between free energies of the more stable diastereoisomeric transition-state pairs, e.g.  $\Delta G_{TS}^{\ddagger} = e\text{-TS}_{rr} - a\text{-TS}_{ss}$ .<sup>17,18b,18c</sup>

For these three reagents the equilibrating rate constants  $k_{ab}$  and  $k_{ba}$  are many orders of magnitude greater than any of the specific rate constants for the formation of the diastereomeric transition-states, and the rates of formation of the more favorable transition-state pairs are more than ten times faster than the rates of their less favorable diastereomeric transition-state pairs (see Table 2).<sup>19</sup> According to Figure 6, the  $\Delta G_{TS}^{\ddagger}$  for these three reactions were 3.78, 2.46, and 2.06 kcal/mol. It follows, therefore, that the first two of these reagents, *B-Ipc-9-BBN* and *B-Ipc-Ipc-BCl*, reduce acetophenone

**Table 1.** Observed and calculated enantioselectivities in the reduction of acetophenone with *B*-Ipc-9-BBN and *B*-*R*-IpcBCl reagents<sup>a</sup>

<i>B</i> - <i>R</i>	PhCH(OH)Me, % ee (Configuration)	
	Observed <sup>b</sup>	Calculated
( <i>B</i> -Ipc-9-BBN)	87 <sup>c</sup> ;100 <sup>d</sup> (S)	99 (S)
Me-	14.5 (S)	13 (S) <sup>e</sup>
Et-	33 (S)	44 (S) <sup>e</sup>
<i>i</i> -Pr-	81 (S)	84 (S) <sup>f</sup>
Cyp-	84 (S)	85 (S) <sup>f</sup>
Ipc-	98 (S)	99 (S) <sup>g</sup>
<i>t</i> -Bu-	96 (R)	97 (R) <sup>g</sup>
Thx-	83 (R) <sup>h</sup>	99 (R) <sup>g</sup>

<sup>a</sup> See text for details. <sup>b</sup> From reference 1. <sup>c</sup> Neat, r.t., from ref. 6g. <sup>d</sup> 6000 atm. from ref. 6d.

<sup>e</sup> Using eq 7; see text. <sup>f</sup> Using eq 6. <sup>g</sup> Using eq 4. <sup>h</sup> Very slow reaction, some product could have been formed via dehydroboration/reduction side reaction.

almost exclusively to the (*S*)-alcohol (99.6% ee (*S*) and 98.6 ee (*S*), respectively, as compared to the experimentally observed 100% ee (*S*)<sup>6g,6d</sup> and 98% ee (*S*).<sup>1c</sup> Evidently, these two reagents react almost exclusively through their **B** conformations *via* the flattened chair transition-states a-TS<sub>s</sub> and a-TS<sub>ss</sub>, rather than through the conformations **A** *via* boat transition-states e-TS<sub>s</sub> and e-TS<sub>rs</sub> as would be expected from the original transition-state model.

On the other hand, in the reduction with the *B*-*t*-Bu-IpcBCl,  $\Delta G_{TS}^{\ddagger} = a-TS_{rs} - e-TS_{sr} = 2.06$  kcal/mol (see Figure 6); in this case the calculated 97 ee% (*R*) compares to the 96% ee (*R*) observed experimentally.<sup>1c</sup> Here, the (*R*)-alcohol originates almost exclusively from the conformation **A** *via* the half-chair e-TS<sub>sr</sub> transition-state. The original model predicts the (*S*) alcohol *via* the diastereomeric boat 'e-TS<sub>ss</sub>' transition-state.

#### *Why are the reactivities of the analogous conformations in the BIpcXY reagents so vastly different?*

Figure 6 show schematic energy differences among various reactive species for the three representative reagents. The **A** and **B** conformations of the *B*-Ipc-9-BBN reagent, (XY=9-BBN, or X=Y), are almost equally populated and yet the acetophenone reacts exclusively with the **B** *via* flattened chair transition-state a-TS<sub>s</sub>. In the *B*-Ipc-IpcBCl reagent, the **A** outnumbers **B** almost 20:1 (and in the other *B*-*prim*- and *B*-*sec*-alkyl-IpcBCl reagents where the **A**:**B** ratio was as high as 36:1 and as low as 1.7:1), acetophenone again reacted predominantly with the *less populated B* *via* flattened chair transition-state a-TS<sub>ss</sub>. On the other hand, in the *B*-*tert*-alkyl-IpcBCl reagents, where the **A** outnumbers **B** 640:1, (*B*-*t*-Bu), and 5555:1, (*B*-Thx), the acetophenone reacts almost exclusively with the *more stable A* *via* a half-chair transition-state e-TS<sub>sr</sub> (and not, as it may be expected from the original model, *via* a boat like e-TS<sub>ss</sub> or *via* half-chair a-TS<sub>rs</sub>, although in either of these two transition-states the 1,3-syn interaction of the C<sub>2</sub>-Me group would involve the C-Me rather than the C-Ph group). *Why?*

#### *B*-Ipc-9-BBN reagent

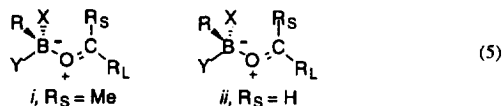
As in the case of the benzaldehyde's reduction,<sup>7</sup> the main reason why the **B** conformation of the *B*-Ipc-9-BBN is more reactive than the **A** is that the overall B-sp<sup>2</sup> → B-sp<sup>3</sup> process for this reagent requires less energy from **B** than from **A**. In other words, developing intermolecular syn-1,3-steric interactions between the R<sub>S</sub>-group of the incoming carbonyl compound with the B-X and B-R groups of the borane reagent in eq 5 provide substantially larger opposition to the B-O bond formation when R<sub>S</sub>=Me, or other alkyl as in *i*, than when R<sub>S</sub>=H, as in *ii*. This appears to be the main reason why the reduction of ketones with this reagent is so much slower than the reduction of aldehydes.

**Table 2.** Heats of formation for relevant stationary points and enthalpies of activation from intrinsic reaction coordinates for the predominant diastereomeric reaction pathways in the reduction of acetophenone with *B*-Ipc-9-BBN and *B*-R-IpcBCl reagents<sup>a</sup>

Conformations, $H_f^b$			Heats of Formation, $H_f^b$					Enthalpies of Activation <sup>c</sup>				
R-B Most Stable <sup>d</sup> Reacting <sup>e</sup>	$K_{AB}^f$	$x$ -B <sub>2</sub> C <sub>2</sub> <sup>g</sup>	Reactants <sup>h</sup>	$x$ -CD <sub>2</sub> <sup>i</sup>	$x$ -TS <sub>int</sub> <sup>j</sup>	Products <sup>k</sup>	$x$ - $\Delta H_{int}^{kl}$	$(x-k_{int})^m$	$x$ - $\Delta H_{int}^{kl}$	$x$ - $\Delta H_{int}^o$		
Ipc <sup>n</sup>	-24.41	A (-24.17)	1.31x10 <sup>1</sup>	e-(R)	-39.18	-28.81	6.56	-73.37	45.74	(1.75x10 <sup>-21</sup> )	35.37	10.37
				e-(S)	-39.18	-23.77	12.92	52.10	(3.79x10 <sup>-26</sup> )	36.69	15.41	
		B (-24.33)		a-(S)	-39.34	-31.61	2.78	42.12	(7.92x10 <sup>-19</sup> )	34.39	7.73	
				a-(R)	-39.34	-29.14	5.66	45.00	(6.11x10 <sup>-21</sup> )	34.80	10.20	
Me-	-42.05	A (-41.84)	6.02x10 <sup>-1</sup>	e-(RR)	-56.85	-54.36	-19.99	-70.17	36.86	(1.74x10 <sup>-20</sup> )	34.37	2.49
				e-(RS)	-56.85	-53.04	-18.64	38.21	(1.13x10 <sup>-21</sup> )	34.40	3.81	
		B (-41.59)		a-(SS)	-56.60	-55.39	-22.62	33.98	(6.01x10 <sup>-18</sup> )	33.98	1.21	
				a-(SR)	-56.60	53.98	-21.14	35.46	(2.98x10 <sup>-19</sup> )	34.46	2.62	
Et-	-47.36	A (-47.10)	8.76x10 <sup>-2</sup>	e-(RR)	-62.11	-59.07	-24.75	-78.15	37.36	(6.08x10 <sup>-21</sup> )	34.32	3.04
				e-(RS)	-62.11	-57.71	-23.41	38.70	(4.18x10 <sup>-22</sup> )	34.30	4.40	
		B (-45.90)		a-(SS)	-60.91	-60.19	-26.70	34.21	(3.77x10 <sup>-18</sup> )	33.49	0.91	
				a-(SR)	-60.91	-58.62	-25.33	35.58	(2.34x10 <sup>-19</sup> )	33.29	2.29	
<i>t</i> -Pr-	-49.64	A (-49.51)	2.78x10 <sup>-1</sup>	e-(RR)	-64.52	-61.28	-26.94	-81.09	37.58	(4.05x10 <sup>-21</sup> )	34.34	3.24
				e-(RS)	-64.52	-60.19	-25.63	38.89	(2.84x10 <sup>-22</sup> )	34.56	4.33	
		B (-48.88)		a-(SS)	-63.98	-62.13	-28.82	35.07	(6.59x10 <sup>-19</sup> )	33.31	1.76	
				a-(SR)	-63.98	-60.66	-27.47	36.42	(4.26x10 <sup>-20</sup> )	33.19	3.23	
Cyp-	-54.70	A (-54.21)	2.81x10 <sup>-2</sup>	e-(RR)	-69.22	-65.40	-31.50	-85.51	37.72	(3.05x10 <sup>-21</sup> )	33.90	3.82
				e-(RS)	-69.22	-	-30.23	39.00	(2.27x10 <sup>-22</sup> )			
		B (-52.45)		a-(SS)	-67.46	-66.31	-33.50	33.96	(6.26x10 <sup>-18</sup> )	32.81	1.15	
				a-(SR)	-67.46	-65.03	-32.16	35.30	(4.13x10 <sup>-19</sup> )	32.87	2.43	
Ipc-	-31.97	A (-31.95)	5.07x10 <sup>-2</sup>	e-(RR)	-46.96	-42.21	-8.48	-63.71	38.48	(6.53x10 <sup>-22</sup> )	33.73	4.75
				e-(RS)	-46.96	-41.41	-7.32	39.64	(6.21x10 <sup>-22</sup> )	34.09	5.55	
		B (-30.48)		a-(SS)	-45.49	-43.38	-10.94	34.55	(1.89x10 <sup>-18</sup> )	32.44	2.11	
				a-(SR)	-45.49	-42.02	-9.49	36.00	(9.98x10 <sup>-20</sup> )	32.53	3.47	
<i>t</i> -Bu-	-49.65	A (-49.25)	1.56x10 <sup>-3</sup>	e-(SR)	-64.26	-60.14	-26.55	-81.39	37.71	(3.11x10 <sup>-21</sup> )	33.59	4.12
				e-(SS)	-64.26	-58.87	-25.19	39.07	(1.97x10 <sup>-22</sup> )	33.68	5.39	
		B (-46.07)		a-(RS)	-61.08	-56.75	-24.49	36.59	(3.02x10 <sup>-20</sup> )	32.26	4.33	
				a-(RR)	-61.08	-57.08	-23.76	37.32	(6.86x10 <sup>-21</sup> )	33.32	4.00	
Thx-	-57.45	A (-57.45)	1.80x10 <sup>-4</sup>	e-(RS)	-72.46	-63.41	-31.46	-89.16	41.00	(5.19x10 <sup>-18</sup> )	31.95	9.05
				e-(SS)	-72.46	-62.66	-30.51	41.95	(1.04x10 <sup>-18</sup> )	32.15	9.80	
		B (-52.93)		a-(RS)	-67.94	-61.95	-28.76	39.18	(1.12x10 <sup>-16</sup> )	33.19	5.99	
				a-(RR)	-67.94	-62.42	-28.65	39.29	(9.33x10 <sup>-17</sup> )	33.80	5.52	

<sup>a</sup> See text for the discussion and explanations. <sup>b</sup> Heats of formation are calculated values from the corresponding optimized geometries. <sup>c</sup> Enthalpies of activation for the formation of the charge-dipole complexes and the corresponding transition-states based on the heats of formation of the reactants (see the *h* below). <sup>d</sup> The most stable conformation does not necessarily correspond to the reacting conformation. <sup>e</sup> Only the two, (A and B), of four possible reacting conformations are included in the Table (see text). <sup>f</sup> The equilibrium constant between conformations A and B. In all cases the reacting conformations can interconvert without the "barrier" (see text). This means that when the  $K_{AB}$  is defined in terms of the rates of transformation, the less stable conformation will undergo conformational inversion to the more stable one at the maximum rate, corresponding to the pre-exponential rate constant factor (see also the *m* below). <sup>g</sup> Description of the reaction pathway; the prefix *x* identifies either *equatorial*, (e-), or *axial*, (a-), approach of acetophenone, and the *mn* subscripts identify either the (R)- or (S)-configurations of the tetragonal boron and the developing chiral carbon centers in the resulting CD<sub>mn</sub> intermediates and in the transition-states TS<sub>mn</sub>. For example the a-(SR) identify the reaction pathway where the acetophenone approaches the chloroborane from the *axial* side of the Ipc ring to give the a-CD<sub>mn</sub> complex intermediate where the *s* identifies the configuration of the tetragonal boron center and *r* identifies the configuration of the chiral carbon center developing from the prochiral carbonyl carbon. <sup>h</sup> Heats of formation of the reacting species, i.e., a heat of formation of the reacting conformation plus the heat of formation of acetophenone (15.01 kcal/mol). <sup>i</sup> CD<sub>mn</sub> and TS<sub>mn</sub> stand for the Charge-Dipole intermediate complexes and the corresponding transition-states. <sup>j</sup> Product stands for the separated chloroborate alcoholate component and the generated  $\alpha$ -pinene. <sup>k</sup>  $\Delta H_{int}^{kl}$  is enthalpy of activation for the formation of transition-state starting from the reacting conformation. <sup>l</sup> Rate constants in *sec*<sup>-1</sup> based on the enthalpy of activation  $\Delta H_{int}^{kl}$  (e.g.,  $a-k_t = \tau(kT/h)e^{-\Delta H_{int}^{kl}/RT}$  where  $\tau$  is the transmission coefficient, assumed to be 1, and  $k$  and  $h$  are the Boltzmann and Planck's constants). <sup>m</sup> Activation enthalpies for the formation of the transition-states from the CD complex. <sup>n</sup> Activation enthalpies for the formation of the CD complex starting from the reacting conformation and acetophenone, assumed to be at least as high as the corresponding enthalpy of formation. <sup>o</sup> *B*-Ipc-9-BBN.

R = Ipc, BXY = 9-BBN, i.e., X = CH, Y = CH



### B-Alkyl-IpcBCl reagents

Based on the energy changes summarized in Figure 6, the main difference between *B*-Ipc-9-BBN and other *B*-R-IpcBCl reagents is that the B-sp<sup>2</sup> → B-sp<sup>3</sup> coordination expansion is opposed by

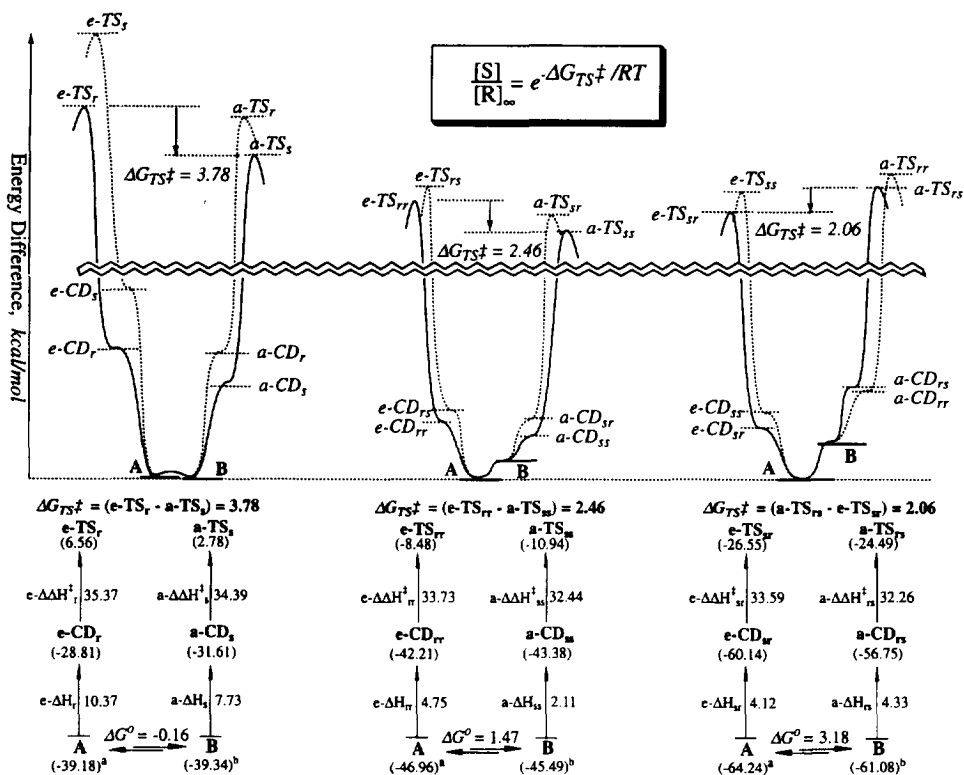
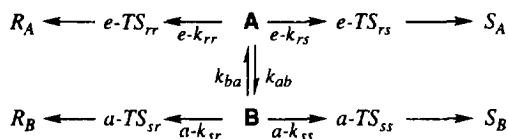


**Figure 6.** Energy diagrams showing relative energies (in kcal/mol) of the reactants, charge-dipole complexes (CDs), and transition-states (TSS) for the reduction of acetophenone with *B*-Ipc-9-BBN (left), *B*-IpcBCl (middle), and with *B*-*t*-Bu-IpcBCl (right). Dashed curves show the less favored pathways from each conformation. The expression in the caption correlates the ratio of the enantiomeric 1-phenylethanols and the energy differences,  $\Delta G_{TS}^{\ddagger}$ , between more favourable diastereomeric transition-states. The bottom part of the figure shows numerical values for the two more favorable pathways. The a and b superscripts identify starting heats of formation of the reactants (i.e. heat of formation of the A or B conformations plus the heat of formation of acetophenone).



**Scheme 3.**

the rigid 9-BBN bicyclic ring system in the former,<sup>7</sup> and by the mobile, flexible structures in the latter. Within the *B*-R-IpcBCl system, the reagents with *primary* or *secondary* *B*-R alkyl groups are apparently more reactive than their *B*-*tert*-alkyl counterparts because they can more readily adjust their internal geometries to accommodate developing steric interactions not only during formation of the diastereomeric CD complexes, but also subsequently, during conversion of the CD complexes to the diastereoisomeric transition-states.

#### Relative importance of the $B-sp^2 \rightarrow B-sp^3$ and $C-sp^2 \rightarrow C-sp^3$ processes

The differences in activation energies for the conversion of the CD intermediates to the corresponding transition-states in the diastereomeric reaction pathways,  $e-\Delta\Delta H^{\ddagger}$  and  $a-\Delta\Delta H^{\ddagger}$ , for all three reagents were less than 4% (see Table 2 and Figure 6). Since in all CD intermediates the pyramidalization at the prostereogenic carbonyl carbon was essentially undetectable, it appears that the overall transition-

state energy difference among diastereomeric pathways,  $\Delta G_{TS}^\ddagger$ , is almost completely due to the energy difference for the formation of the diastereomeric CD intermediates. In other words, the stereoselectivity of the reduction is mainly controlled by the  $B\text{-sp}^2 \rightarrow B\text{-sp}^3$  process during formation of the first of the two new transition-state stereogenic centers; the  $C\text{-sp}^2 \rightarrow C\text{-sp}^3$  process, leading to the formation of the second transition-state stereogenic center, apparently contributes very little to the overall stereoselectivity control.

#### Contribution of torsional strain to stereoselectivity control

The summarized energy changes in Figure 6 illustrate graphically how torsional strain contributes to the stereoselectivity control. First, for the *B*-Ipc-9-BBN, the  $A \rightarrow e\text{-CD}_T$  process requires about 2.6 kcal/mol *more* energy than the  $A \rightarrow B \rightarrow a\text{-CD}_S$  one. Evidently, in both reaction pathways the torsional energy for the  $A \rightarrow B$  interconversion is only a small fraction of the total energy,<sup>19</sup> and therefore the preference for the  $A \rightarrow B \rightarrow a\text{-CD}_S$  process is almost entirely due to the higher reactivity of the **B** conformation.

In the *B*-Ipc-IpcBCl the **A** outnumbers **B** almost 20:1 and yet acetophenone reacts almost exclusively with **B** via  $a\text{-CD}_{SS}$ . This molecule (and presumably other reagents with a *secondary* or *primary* *B*-R group), can choose the indirect pathway,  $A \rightarrow B \rightarrow a\text{-CD}_{SS}$ , over the less favorable direct one,  $A \rightarrow e\text{-CD}_{IT}$ , by rotating from the more stable but less reactive **A** to the less stable but more reactive **B** before engaging in the reaction with the carbonyl substrate. The energy of the  $A \rightarrow a\text{-CD}_{SS}$  overall process, which includes torsional energy for the  $A \rightarrow B$  rotation, is still by 1.17 kcal/mol lower than the energy of the direct  $A \rightarrow e\text{-CD}_{IT}$  process.

On the other hand, when *B*-R=*tert*-alkyl, e.g. *t*-Bu, a direct  $A \rightarrow e\text{-CD}_{SR}$  process requires 3.4 kcal/mol *less* energy than the  $A \rightarrow B \rightarrow a\text{-CD}_{RS}$  transformation. In other words, if the *B*-*t*-Bu-IpcBCl is to follow the  $A \rightarrow B \rightarrow a\text{-CD}_{RS}$  pathway, the **A** would have first to overcome the 3.18 kcal/mol  $A \rightarrow B$  torsional strain — about 77% of the total energy for the direct  $A \rightarrow e\text{-CD}_{SR}$  process — just to get to **B**, and then it would need another 4.3 kcal/mol to get from **B** to  $a\text{-CD}_{RS}$ . As mentioned above, the larger torsional strain in the *B*-*tert*-alkyl-IpcBCl relative to the *B*-*prim*- and *B*-*sec*-alkyl-IpcBCl reagents (including *B*-Ipc-9-BBN), is due to unavoidable interactions of the sterically demanding *B*-*tert*-alkyl groups with the  $C_1\text{--}C_6$  bond of the Ipc ring during the  $A \rightarrow B$  rotation, and is apparently the main reason for the reversal in the reactivities of the **A** and **B** conformations of the *B*-*tert*-alkyl-IpcBCl reagents.

We will only briefly discuss the reductions with other *B*-R-IpcBCl reagents.

#### *B*-Thx-IpcBCl

With this reagent a direct  $A \rightarrow e\text{-CD}_{SR}$  pathway requires 1.46 kcal/mol less energy than the  $A \rightarrow B \rightarrow a\text{-CD}_{RS}$  transformation (see Table 2). In the  $A \rightarrow B \rightarrow a\text{-CD}_{RS}$  pathway, the **A** would have first to overcome the 4.5 kcal/mol  $A \rightarrow B$  torsional strain just to get to **B**, and then it would need another 6 kcal/mol to get from **B** to  $a\text{-CD}_{RS}$ . A substantially slower experimental rate,<sup>1c</sup> relative to the *B*-*t*-Bu-IpcBCl, is apparently due to the higher  $B\text{-sp}^2 \rightarrow B\text{-sp}^3$  pyramidalization energy of the large *B*-Thx group.

#### *B*-Cyp-, *B*-*i*-Pr-, *B*-Et-, and *B*-Me-IpcBCl

In their evaluations of the conformationally mobile reaction systems, Zefirov<sup>17</sup> and Seeman<sup>18b</sup> discussed the 'boundary conditions' for the application of the Curtin–Hammett principle and for the use of the above eq 4 and 4a for the product distribution determination. They also reviewed kinetically more complicated 'multi-component systems' and other mathematical expressions for the determination of the product distribution under these conditions. It appears that the experimentally observed products ratio<sup>1c</sup> in the reductions with the *B*-*sec*-alkyl reagents *B*-Cyp-, and *B*-*i*-Pr-, is better described by eq 6,  $[S]_\infty/[R]_\infty = (e^{-k_S} + a \cdot k_S \cdot K) / (e^{-k_T} + a \cdot k_T \cdot K)$ , the expression used previously, for example, in the analysis of the reduction of conformationally mobile cyclohexanones with lithium aluminum hydride.<sup>18e</sup> The

calculated values in Table 1 for the (*S*)-1-phenylethanol, 85% ee for the *B*-Cyp and 84% ee for the *B*-*i*-Pr reagents, were obtained using eq 6 and the appropriate rate constants from Table 2.

As the difference in the sizes of the B–X and B–Y groups decreases, the contribution of the alternate reaction pathways to the overall product distribution increase and the above mathematical expressions for the  $[S]_{\infty}/[R]_{\infty}$  no longer accurately reflect the true kinetic behavior of such systems. In such situations, the product ratio  $[S]_{\infty}/[R]_{\infty}$  could be estimated from the difference in free energies of *all* diastereomeric transition-states<sup>18b</sup> participating in the reaction, i.e.  $[S_A+S_B]_{\infty}/[R_A+R_B]_{\infty}=(H_{RA}+H_{RB})-(H_{SA}+H_{SB})$ , (eq 7), where  $H_{RA}$  through  $H_{SB}$  are calculated heats of formation of the respective transition-states (see Scheme 2 and Table 2). The calculated enantiomeric excess for the *B*-Me and *B*-Et reagents in Table 1, (ee (*S*))=13% and 44%, respectively), were obtained by using eq 7. It should be recognized that the *B*-Et substituent and higher *prim*-alkyl groups, could assume three alternate conformations relative to the BIpcCl which would contribute differently to the overall composition of the diastereomeric transition-states. This is probably the main reason for relatively large discrepancy between the experimentally observed and calculated ee values for the *B*-Et reagent.

### The origins of stereoselectivity

The models show that for either e-CD or a-CD complex to get to the transition-state, the C<sub>2</sub>-hydrogen must get to the bonding distance of the carbonyl carbon (cf the atom distances  $d_3$  in Figure 4). For this to happen, the entire Ipc ring had to rotate about the B–C<sub>1</sub> bond clockwise in the e-CD complexes and counterclockwise in a-CD (see  $\omega_2$  and  $\omega_3$  in Figure 4).

The other geometrical parameters in Figure 4 illustrate the extent of the pyramidalization at the prostereogenic boron and carbon centers at different stages of the reaction coordinate. As evident from Figs 4 and 5, during formation of the *new B–O bond*, the B-sp<sup>2</sup> to B-sp<sup>3</sup> coordination expansion forces either *sterically more demanding* C<sub>1</sub>–C<sub>6</sub> bond or *sterically less demanding* C<sub>1</sub>–H bond gauche to the B–Y and B–X bonds. Subsequently, in the *second phase of the reaction*, during conversion of the CD complexes to transition-states and the C-sp<sup>2</sup> to C-sp<sup>3</sup> coordination expansion, the required rotation about the B–C<sub>1</sub> bond forces again either the sterically more demanding C<sub>1</sub>–C<sub>6</sub> or sterically less demanding C<sub>1</sub>–H bond toward the B–X bond.

The unequal increase of the steric strain in these processes, and hence the observed stereoselectivity in the borane reductions, is another manifestation of the steric phenomena observed in addition reaction of simple nucleophiles<sup>20</sup> to carbonyl double bonds as described in the Felkin–Anh model.<sup>8a–f</sup> In such addition reactions, due to the absence of the prostereogenic center within the nucleophilic reagent, the model<sup>8a–f</sup> considers observed stereoselectivities to be a result of the developing steric interactions only among the substituents in the prostereogenic carbonyl substrate, during the C-sp<sup>2</sup> → C-sp<sup>3</sup> coordination expansion process. Since in these simple systems the C-sp<sup>2</sup> → C-sp<sup>3</sup> coordination provides the first and only new stereogenic center, this process, *de facto*, controls the overall stereochemical outcome of the reaction.

In the borane reductions, however, the prostereogenic boron reaction center provides additional diastereomeric reaction pathways. The B-sp<sup>2</sup> → B-sp<sup>3</sup> process *in the reagent* chronologically precedes the C-sp<sup>2</sup> → C-sp<sup>3</sup> one *in the substrate* and, thus, it appears to control the stereoselectivity of the overall reaction. The just reported results of the acetophenone reductions with borane reagents containing *increasingly larger alkyl substituents* support this contention.

### Conclusions

The AM1 calculations corroborate an *a priori* conformational analysis conclusion about the reactivities of the borane reagent's conformations and support the experimental observations<sup>2a–c,4a,6a,15,21</sup> that the reductions of the carbonyl group probably involve charge–dipole complexes as the reaction intermediates. On the other hand, contrary to the earlier transition-state model, the calculations show that the respective transition-states resemble half-chairs and flattened-chairs rather than a boat form,

and clarify a role of the *B*-*R* group in determining the reagent's stereoselectivity. Furthermore, unlike the original model, which stipulates that the stereoselectivity is determined by preferential 1,3-syn interactions between the C-*R*<sub>S</sub> bond of the carbonyl substrate with the C<sub>2</sub>-Me group of the reagent, the present calculations show that the preferred reaction pathway is mainly controlled by the 1,3-syn interactions between the substrate's C-*R*<sub>S</sub> bond and the B-Cl bond of the reagent, *during formation of the initial charge-dipole complex*.

Aside from the differences with the original model, the present interpretation of the origins of the stereoselectivity in these reductions recognizes the importance of the developing steric interactions during coordination expansion of the prostereogenic centers both in the nucleophilic borane reagent and in the electrophilic carbonyl substrate. In fact, since the B-sp<sup>2</sup> → B-sp<sup>3</sup> process in the nucleophilic reagent chronologically precedes the C-sp<sup>2</sup> → C-sp<sup>3</sup> one in the carbonyl substrate, it seems that the interactions in the former one are primarily responsible for the overall stereochemical outcome of the reaction. Therefore, unlike in addition reactions of simple nucleophiles to prostereogenic carbonyl carbon where the stereoselectivity is controlled *by the structure of the substrate*, in the reductions with prostereogenic boron reagents, the stereoselectivity should be mainly controlled *by the structure of the reagent itself*. Nevertheless, it will be of interest to determine the generality of this conclusion and to establish with a broader range of the *R*<sub>S</sub> and *R*<sub>L</sub> substituents in the substrate how the B-sp<sup>2</sup> → B-sp<sup>3</sup> and C-sp<sup>2</sup> → C-sp<sup>3</sup> processes individually contribute to the overall stereoselectivity in the reduction, which one plays a dominating role, and what kinds of structural changes in the nucleophilic and electrophilic components of the reaction system, i.e. in the reagent on the one hand and in the substrate on the other, may reverse if at all, their relative importance.

### Acknowledgements

MMR gratefully acknowledges generous hardware/software gifts from the CAChe Scientific — the Oxford Molecular Modeling Company — which made this study possible.

### References

1. See for example (a) Brown, H. C.; Ramachandran, P. V. in Hassner, A. Ed. *Advances in Asymmetric Synthesis* Vol. 1, JAI Press, Greenwich, CT, **1995**, pp. 147–210. (b) Brown, H. C.; Ramachandran, P. V. *J. Organomet. Chem.* **1995**, *500*, 1. (c) Brown, H. C.; Ramachandran, P. V. *Acc. Chem. Res.* **1992**, *25*, 16.
2. (a) Midland, M. M.; Tramontano, A.; Zderic, S. A. *J. Am. Chem. Soc.* **1977**, *99*, 5211. (b) Midland, M. M.; Greer, S.; Tramontano, A.; Zderic, S. A. *J. Am. Chem. Soc.* **1979**, *101*, 2352. (c) Midland, M. M.; Zderic, S. A. *J. Am. Chem. Soc.* **1982**, *104*, 525. (d) Midland, M. M.; Tramontano, A.; Zderic, S. A. *J. Organomet. Chem.* **1978**, *156*, 203.
3. (a) Midland, M. M.; McDowell, D. C.; Hatch, R. L.; Tramontano, A. *J. Am. Chem. Soc.* **1980**, *102*, 867. (b) Midland, M. M.; McLoughlin, J. I. *J. Org. Chem.* **1984**, *49*, 1317. (c) Midland, M. M.; Tramontano, A.; Kazubski, A.; Graham, R. S.; Tsai, D. J. S.; Cardin, D. B. *Tetrahedron* **1984**, *40*, 1371. (d) See also, Ramachandran, P. V.; Teodorovic, A. V.; Rangaishenvi, M. V.; Brown, H. C. *J. Org. Chem.* **1992**, *57*, 2379.
4. (a) Brown, H. C.; Ramachandran, P. V.; Chandrasekharan, J. *Organometallics*, **1986**, *5*, 2138 (b) Brown, H. C.; Chandrasekharan, J.; Ramachandran, P. V. *J. Am. Chem. Soc.* **1988**, *110*, 1539. (c) Brown, H. C.; Srebnik, M.; Ramachandran, P. V. *J. Org. Chem.* **1989**, *54*, 1577. (d) Brown, H. C.; Ramachandran, P. V. *J. Org. Chem.* **1989**, *54*, 4504. (e) Brown, H. C.; Ramachandran, P. V.; Teodorovic, A. V.; Swaminatham, S. *Tetrahedron Lett.* **1991**, *32*, 6691. (f) Joshi, N. N.; Pyun, C.; Mahindroo, V. K.; Singram, B.; Brown, H. C. *J. Org. Chem.* **1992**, *57*, 504.
5. (a) Ramachandran, P. V.; Teodorovic, A. V.; Rangaishenvi, M. V.; Brown, H. C. *J. Org. Chem.* **1992**, *57*, 2379. (b) Ramachandran, P. V.; Teodorovic, A. V.; Brown, H. C. *Tetrahedron* **1993**, *49*, 1725.

6. (a) Mikhailov, B. M.; Bubnov, Yu. N.; Kiselev, V. G. *J. Gen. Chem. USSR (Engl. Transl.)* **1966**, 36, 65. (b) For a general discussion and literature review, see Morrison, J. D.; Mosher, H. S. *Asymmetric Organic Reactions* American Chemical Society, Washington, DC, **1976**, Chapter 5.
7. Rogic, M. M. *J. Org. Chem.* **1996**, 61, 1341.
8. (a) Cherest, M.; Felkin, H.; Prudent, N. *Tetrahedron Lett.* **1968**, 2199. (b) Cherest, M.; Felkin, H. *Tetrahedron Lett.* **1968**, 2205. (c) Anh, N. T.; Eisenstein, O. *Nouv. J. Chem.* **1977**, 1, 61. (d) Anh, N. T. *Fortschr. Chem. Forschung.* **1980**, 88, 145. (e) Wu, Y.-D.; Tucker, J. A.; Houk, K. N. *J. Am. Chem. Soc.* **1991**, 113, 5018. (f) Wu, Y.-D.; Houk, K. N.; Florez, J.; Trost, B. M. *J. Org. Chem.* **1991**, 56, 3656, and references therein. For a general discussion see also ref. 13a, pp. 875–888.
9. (a) Dewar, M. J. S.; Zoebisch, E. G.; Healy, E. F.; Stewart, J. J. P. *J. Am. Chem. Soc.* **1985**, 107, 3902. Liotta<sup>9b</sup> used MNDO method to similarly evaluate enantioselectivity in oxazaborolidine-catalyzed reductions of ketones, and Houk *et al.*, in their earlier work, investigated stereoselectivities of various hydroborating reagents<sup>9c–e</sup> and in a more recent one<sup>9f–g</sup> investigated stereoselectivities of the reductions of ketones and conformational analysis of chiral alkenes and oxonium ions using ab initio calculations; they developed an improved MM2 force field which qualitatively reproduces observed stereoselectivities: (b) Jones, D. K.; Liotta, D. C.; Shinkai, I.; Mathre, D. J. *J. Org. Chem.* **1993**, 58, 799. (c) Houk, K. N.; Rondan, N. G.; Wu, Y. D.; Metz, J. T.; Paddon-Row, M. N. *Tetrahedron* **1984**, 40, 2257. (d) Houk, K. N.; Paddon-Row, M. N.; Rondan, N. G.; Wu, Y. d.; Brown, F. K.; Spellmeyer, D. C.; Metz, J. T.; Li, Y.; Loncharich, R. J. *Science* **1986**, 231, 1108. (e) Masamune, S.; Kennedy, R. M.; Petersen, J. S.; Houk, K. N.; Wu, Y. D. *J. Am. Chem. Soc.* **1986**, 108, 1986. (f) Eksterowez, J. E.; Houk, K. N. *Chem. Rev.* **1993**, 93, 2439. (g) Broeker, J. L.; Hoffmann, R. W.; Houk, K. N. *J. Am. Chem. Soc.* **1991**, 113, 5006.
10. (a) CAChe Scientific — the Oxford Molecular Modeling Co. — Beaverton, OR 97077. (b) Clark, T. A. *Handbook of Computational Chemistry* J. Wiley and Sons, New York, **1985**. (c) Baker, J. J. *Comput. Chem.* **1986**, 7, 385.
11. (a) Dewar, M. J. S.; Healy, E. F.; Stewart, J. J. P. *J. Chem. Soc., Faraday Trans. 2*, **1984**, 3, 227. (b) Dewar, M. S. J.; Kirschner, S. *J. Am. Chem. Soc.* **1971**, 93, 4290. (c) McIver, J.; Komornicki, A. *ibid.* **1972**, 94, 2625.
12. (a) Midland and coworkers documented exclusive involvement of the C<sub>2</sub>-hydrogen from the Ipc ring in the these reductions.<sup>2b</sup> See also ref. 4f. (b) The arguments why the reaction pathways based on the C and F conformations are not important were presented in reference 7.
13. (a) For the distinction between a conformation and a conformational isomer or conformer, see Eliel, E. L.; Wilen, S. H. *Stereochemistry of Organic Compounds* John Wiley and Sons, New York, **1994**, p. 597. (b) p. 1200. (c) Eliel, E. L. *Stereochemistry of Carbon Compounds* McGraw-Hill, New York, **1962**, pp. 149–152.
14. (a) As before<sup>7</sup> it is assumed that the *relative* calculated energies in the gas phase would reasonably approximate those in solution or under neat conditions. (b) For a brief discussion how (in a relatively simple molecule) various factors contribute to torsional potential, see ref. 13a, p. 614 and references therein.
15. Li, Y.; Houk, K. N. *J. Am. Chem. Soc.* **1989**, 111, 1236. In his ab initio calculations of transition-states for the reaction of formaldehyde with allylborane and allylboronic acid, Houk also identified an allylborane–aldehyde complex in which ‘the boron is coordinated with an in-plane lone-pair on oxygen in both the complex and in the chair transition structure’. In this complex too the pyramidalization at the boron center was already in progress, while there was no appreciable change at the carbonyl carbon. See also ref. 9g.
16. From the electronic point of view the organoborane reductions could be considered (4+2) processes where the borane agent and the carbonyl compound appear (by analogy to other MPV type reductions from eq 1), as ‘diene’ and dienophile or as a *nucleophile* and *electrophile*. For example, according to AM1, the HOMO/LUMO energies of *B*-*t*-Bu-IpcBCl and acetophenone are –10.91/–4.07 eV and –11.28/–8.74 eV, respectively, indicating it is the borane’s HOMO that



interacts with the carbonyl's LUMO and, therefore, the initial charge-dipole interaction involves in-plane  $n$  electron-pair on oxygen rather than the  $\pi$ -electron-pair.

17. (a) Zefirov, N. S.; Palyulin, V. A. *Zh. Org. Chem.* **1979**, *15*, 1098. (b) Zefirov, N. S. *Tetrahedron* **1977**, *33*, 2719.
18. (a) Curtin, D. Y. *Rec. Chem. Prog.* **1954**, *15*, 111. (b) For extensive discussion of the conformation/reactivity relationships, the Curtin-Hammett principle, and kinetic analyses, see Seeman, J. I. *Chem. Rev.* **1983**, *83*, 83. (c) Winstein, S.; Holness, N. J. *J. Am. Chem. Soc.* **1955**, *77*, 5562. (d) Eliel, E. L.; Ro, R. S. *Chem. Ind. (London)* **1956**, 251. (e) Hutchins, R. O. *J. Org. Chem.* **1977**, *42*, 920.
19. For the discussion of the 'boundary conditions' where the Curtin-Hammett treatment and Winstein-Holness equation apply, see ref. 18b and ref. 13a, p. 649.
20. By 'simple nucleophiles' we mean here structures lacking reactive prostereogenic centers.
21. Wieggers, A.; Scharf, H. D. *Tetrahedron: Asym.* **1996**, *7*, 2303. These authors also concluded that the overall reduction is a two-step process and presented the evidence for the involvement of the carbonyl/borane complexes in the first step of the reaction.

(Received in USA 24 February 1997)